XLVI CILAMCE
VITÓRIA - ES - BRAZIL - 2025
XLVI IBERO-LATIN AMERICAN CONGRESS ON COMPUTATIONAL METHODS IN ENGINEERING

An object-oriented framework for FE² multiscale analysis

Elias Saraiva Barroso[1], Luiz Antonio Taumaturgo Mororó[2], Evandro Parente Junior[1], Marcelo Silva Medeiros Júnior[1], João Batista Marques de Sousa Júnior[1], Antônio Macário Cartaxo de Melo[1]

[1]*Departamento de Engenharia Estrutural e Construção Civil, Universidade Federal do Ceará*
Campus do Pici, Bloco 728, 60440-900, Fortaleza/CE-Brazil
elias.barroso@ufc.br, evandro@ufc.br, marcelomedeiros@ufc.br, joaobatistasousajr@ufc.br, macario@ufc.br
[2]*Instituto Federal do Ceará, Campus Fortaleza*
Av. Treze de Maio, 2081 - Benfica, 60040-531, Fortaleza/CE-Brazil
luiz.mororo@ifce.edu.br

Abstract. This work presents the computational implementation of the FE^2 multiscale analysis approach into an academic finite element code developed in C++ using Object-Oriented Programming concepts. In this approach, both the macro and micro levels are discretized in finite elements. Furthermore, the microscale is related to integration points of the macroscale model, and the scale transition is carried out using appropriate averaging theorems and periodic boundary conditions. The software architecture adopted suitable design patterns for FE^2 implementation, which is described using UML diagrams. The implementation is verified by comparing the obtained results with reference solutions available in the literature.

Keywords: Computational Homogenization, Multiscale Analysis, FE^2, Object-Oriented Programming.

1 Introduction

Computational Homogenization (CH) is a technique used to characterize the macroscopic material behavior using a computational Representative Volume Element (RVE). It contrasts with the Analytical Homogenization (AH) strategies, where closed-form mathematical expressions are used (e.g. Rule of Mixtures and Mori-Tanaka) [1–3].

In offline CH approaches, the RVE is used to evaluate the material parameters required by the adopted constitutive model of the macroscale model. Moreover, CH can also be performed on the fly (or online), as a mechanical analysis is performed at the macroscale. In this case, no prior assumptions with respect to the material behavior at the lower level are required, allowing for modeling of complex microscale phenomena that would be difficult or impossible to capture with macroscopic constitutive models homogenized in an offline scheme. The so-called FE^2 multiscale approach uses finite element models for both micro and macro scales [4].

This work addresses the computational implementation of a CH approach based on FE^2 into an academic finite element code developed in C++ using Object-Oriented Programming (OOP) concepts. In the adopted approach, the microscale is related to integration points of the macroscale model and the scale transition is carried out using appropriate averaging theorems and periodic boundary conditions. The software architecture adopted suitable design patterns for FE^2 implementation, which is described using UML diagrams. The computational implementation is verified using a numerical example.

2 Multiscale Analysis

In this section, we present the main theoretical background and computational aspects behind the adopted continuous CH approach for material modeling in a quasi-static setting using the FE^2 framework, without providing all details of the CH approach as presented in literature. Strictly speaking, we follow the works by Perić et al. [5] and Nguyen [6]. The main premise of a CH approach is to determine on the fly the constitutive behavior of a material at the upper scale (i.e., the stress-strain relation, $\boldsymbol{\sigma}_{\mathrm{M}} = f(\boldsymbol{\varepsilon}_{\mathrm{M}})$) from a sample (or samples) of its underlying microstructure at the lower scale. In this context, the material configuration is considered to be sufficiently homogeneous at the upper scale, but heterogeneous at the lower scale [7], i.e., the microstructure may

consist of different constituents with different mechanical behaviors, and cavities with different sizes, for instance.

Fig. 1 schematically illustrates the global solution scheme of the CH approach for obtaining the stress-strain relation which encompasses three main stages. Firstly, for a macroscopic material point $\mathbf{x}_\mathrm{M}$ (i.e., a macroscopic integration point in a finite element setting), its corresponding strain field $\boldsymbol{\varepsilon}_\mathrm{M}$ is passed to its corresponding microscopic sample, i.e., the RVE model, to be used as boundary condition imposed on the external boundary Γ_m defined on the microscopic domain Ω_m. Secondly, the equilibrium of the RVE model with such boundary condition is satisfied by solving the microscopic boundary value problem (BVP). Thirdly, the macroscopic stress $\boldsymbol{\sigma}_\mathrm{M}$ is determined by averaging the microscopic stress $\boldsymbol{\sigma}_\mathrm{m}$ over the volume of the RVE model.

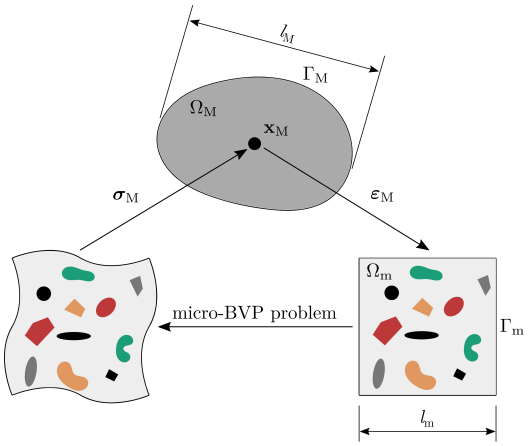


Figure 1. Global solution procedure for the CH approach for a given macroscopic material point $\mathbf{x}_\mathrm{M}$ in order to obtain the constitutive relation $\boldsymbol{\sigma}_\mathrm{M} = f(\boldsymbol{\varepsilon}_\mathrm{M})$. Arrows represent the data exchange among the analysis phases.

2.1 Macroscale formulation

Considering the macroscopic domain of computation Ω_M bounded by Γ_M and subject to Dirichlet and Neumann boundary conditions, as shown in Fig. 1, the equilibrium equation and the relation between the total strain $\boldsymbol{\varepsilon}_\mathrm{M}$ and the displacement field $\mathbf{u}_\mathrm{M}$ without body force read, respectively,

$$\boldsymbol{\nabla}_\mathrm{M} \cdot \boldsymbol{\sigma}_\mathrm{M} = \mathbf{0} \quad \text{or} \quad \sigma^\mathrm{M}_{ij,j} = 0 \quad \text{in} \quad \Omega_\mathrm{M}, \tag{1}$$

and

$$\boldsymbol{\varepsilon}_\mathrm{M} = \frac{1}{2}\left(\nabla_\mathrm{M}\mathbf{u}_\mathrm{M} + (\nabla_\mathrm{M}\mathbf{u}_\mathrm{M})^\mathrm{T}\right) = \nabla^\mathrm{S}_\mathrm{M}\mathbf{u}_\mathrm{M} \quad \text{or} \quad \varepsilon^\mathrm{M}_{ij} = \frac{1}{2}\left(u^\mathrm{M}_{i,j} + u^\mathrm{M}_{j,i}\right), \tag{2}$$

where $\boldsymbol{\sigma}_\mathrm{M}$ is the second-order Cauchy stress tensor. Note that only the symmetric part of $\nabla\mathbf{u}_\mathrm{M}$ is considered, i.e., $\nabla^\mathrm{S}_\mathrm{M}\mathbf{u}_\mathrm{M} = \frac{1}{2}\left(\nabla_\mathrm{M}\mathbf{u}_\mathrm{M} + (\nabla_\mathrm{M}\mathbf{u}_\mathrm{M})^\mathrm{T}\right)$. To complete the macroscopic boundary value problem stated above, a relation between the stress and strain needs to be provided. Instead of using a constitutive model in a closed form, CH techniques obtain such relation numerically via the computational analysis of a RVE.

2.2 Microscale formulation

Like the macroscale formulation described in the previous section, the equilibrium equation and the relation between total strain and the displacement field for the microscopic domain, i.e., in the RVE, are, respectively,

$$\boldsymbol{\nabla}_\mathrm{m} \cdot \boldsymbol{\sigma}_\mathrm{m} = \mathbf{0} \quad \text{in} \quad \Omega_\mathrm{m} \quad \text{and} \quad \boldsymbol{\varepsilon}_\mathrm{m} = \nabla^\mathrm{S}_\mathrm{m}\mathbf{u}_\mathrm{m}. \tag{3}$$

Considering a large length scale separation, $l_\mathrm{m} \ll l_\mathrm{M}$ (Fig. 1), for the principle of separation of scales [4], the $\boldsymbol{\varepsilon}_\mathrm{M}$ is considered uniform over the Ω_m. Thus, without loss of generality, the displacement field at any point $\mathbf{x}_\mathrm{m}$ and at any time t in the microscopic domain can be split as [5]:

$$\mathbf{u}_\mathrm{m}(\mathbf{x}_\mathrm{m}, t) = \boldsymbol{\varepsilon}_\mathrm{M}(\mathbf{x}_\mathrm{M}, t) \cdot \mathbf{x}_\mathrm{m} + \tilde{\mathbf{u}}_\mathrm{m}(\mathbf{x}_\mathrm{m}, t), \tag{4}$$

into a sum of a displacement due to a homogeneous macroscopic strain field contribution, $\boldsymbol{\varepsilon}_\mathrm{M}(\mathbf{x}_\mathrm{M}, t) \cdot \mathbf{x}_\mathrm{m}$, and a displacement fluctuation field contribution, $\tilde{\mathbf{u}}_\mathrm{m}(\mathbf{x}_\mathrm{m}, t)$, which accounts for the heterogeneity of the microstructure

(see Fig. 2). The term $\boldsymbol{\varepsilon}_{\mathrm{M}}(\mathbf{x}_{\mathrm{M}}, t)$ is the macroscopic strain tensor at a given point $\mathbf{x}_{\mathrm{M}}$ at the same time t (see eq. (2)). By substituting eq. (4) into eq. (3), the microscopic strain tensor can also be expressed as:

$$\boldsymbol{\varepsilon}_{\mathrm{m}}(\mathbf{x}_{\mathrm{m}}, t) = \boldsymbol{\varepsilon}_{\mathrm{M}}(\mathbf{x}_{\mathrm{M}}, t) + \tilde{\boldsymbol{\varepsilon}}_{\mathrm{m}}(\mathbf{x}_{\mathrm{m}}, t), \tag{5}$$

where the microscopic strain fluctuation field is defined as $\tilde{\boldsymbol{\varepsilon}}_{\mathrm{m}}(\mathbf{x}_{\mathrm{m}}, t) = \nabla^{\mathrm{S}}_{\mathrm{m}} \tilde{\mathbf{u}}_{\mathrm{m}}$ (see Fig. 2).

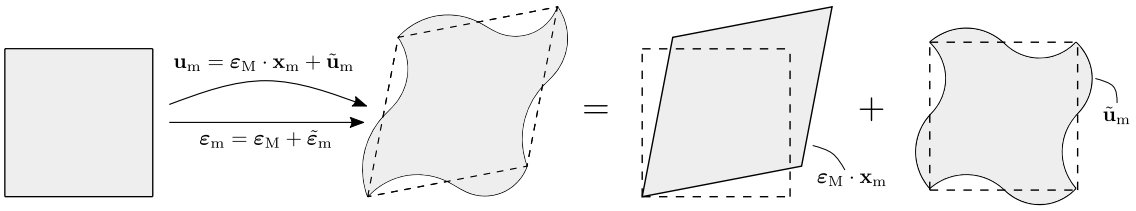


Figure 2. Microscale displacement field.

The mechanical behavior of each microscopic constituent i is assumed to be known and described by phenomenological constitutive models at any time and point in Ω_{m}:

$$\boldsymbol{\sigma}^{i}_{\mathrm{m}}(\mathbf{x}_{\mathrm{m}}, t) = \mathcal{F}^{i}(\boldsymbol{\varepsilon}_{\mathrm{m}}(\mathbf{x}_{\mathrm{M}}, t), \boldsymbol{\alpha}_{\mathrm{m}}(\mathbf{x}_{\mathrm{M}}, t)), \tag{6}$$

where $\mathcal{F}$ represents a general constitutive operator, and $\boldsymbol{\alpha}_{\mathrm{m}}$ are internal variables that store the state of the material.

For completeness, boundary conditions have to be provided to the microscopic problem stated above. The essential step in CH approaches is the application of the RVE boundary conditions for deriving scale transition relations, as discussed in the following.

2.3 Scale transition

Starting with the macro-to-micro downscaling procedure, where $\boldsymbol{\varepsilon}_{\mathrm{M}}$ is passed to the micromodel (see Fig. 1), the averaging theorem for strain is used so that a relation between $\boldsymbol{\varepsilon}_{\mathrm{M}}$ and $\boldsymbol{\varepsilon}_{\mathrm{m}}$ is derived:

$$\boldsymbol{\varepsilon}_{\mathrm{M}}(\mathbf{x}_{\mathrm{M}}, t) = \frac{1}{|\Omega_{\mathrm{m}}|} \int_{\Omega_{\mathrm{m}}} \boldsymbol{\varepsilon}_{\mathrm{m}}(\mathbf{x}_{\mathrm{m}}, t)\, \mathrm{d}\Omega, \tag{7}$$

where $|\cdot|$ represents a measure for the domain, being the area and volume in two and three dimension settings, respectively. By using Gauss theorem for converting a domain integral into a surface one (i.e., from Ω_{m} to Γ_{m} of the RVE) and eq. (3), the expression above can be rewritten in a different form [6]:

$$\varepsilon^{\mathrm{M}}_{ij} = \frac{1}{2|\Omega_{\mathrm{m}}|} \int_{\Gamma_{\mathrm{m}}} \left(u^{\mathrm{m}}_{i} n^{\mathrm{m}}_{j} + u^{\mathrm{m}}_{j} n^{\mathrm{m}}_{i} \right) \mathrm{d}\Gamma, \tag{8}$$

with $\mathbf{n}^{\mathrm{m}}$ being the outward normal vector on Γ_{m} (see Fig. 3). Substituting eq. (4) into eq. (8) yields:

$$\varepsilon^{\mathrm{M}}_{ij} = \varepsilon^{\mathrm{M}}_{ij} + \frac{1}{2|\Omega_{\mathrm{m}}|} \int_{\Gamma_{\mathrm{m}}} \left(\tilde{u}^{\mathrm{m}}_{i} n^{\mathrm{m}}_{j} + \tilde{u}^{\mathrm{m}}_{j} n^{\mathrm{m}}_{i} \right) \mathrm{d}\Gamma. \tag{9}$$

Therefore, in order to guarantee the equality above and, consequently, the strain averaging theorem in eq. (7), independently of a particular $\tilde{\mathbf{u}}_{\mathrm{m}}$, periodic boundary conditions are imposed on the RVE such that the contribution of $\tilde{\mathbf{u}}_{\mathrm{m}}$ vanishes. In this condition, the periodicity of the microfluctuation field is imposed on the RVE boundary such that the microfluctuation on two opposite faces of the RVE, $\Gamma^{+}_{\mathrm{m},i}$ and $\Gamma^{-}_{\mathrm{m},i}$ (see Fig. 3), having the same size and $\mathbf{n}^{+}_{i} = -\mathbf{n}^{-}_{i}$, can be related according to $\tilde{\mathbf{u}}_{\mathrm{m}}(\mathbf{x}^{+}_{\mathrm{m}}) = \tilde{\mathbf{u}}_{\mathrm{m}}(\mathbf{x}^{-}_{\mathrm{m}})$. Observe that such condition adds anti-periodicity in terms of traction, $\mathbf{t}_{\mathrm{m}}(\mathbf{x}^{+}_{\mathrm{m}}) = -\mathbf{t}_{\mathrm{m}}(\mathbf{x}^{-}_{\mathrm{m}})$. Due to such periodicity on $\tilde{\mathbf{u}}_{\mathrm{m}}$, one can write [8]:

$$\mathbf{u}^{+}_{\mathrm{m}} - \mathbf{u}^{-}_{\mathrm{m}} = \boldsymbol{\varepsilon}_{\mathrm{M}} \otimes \left(\mathbf{x}^{+}_{\mathrm{m}} - \mathbf{x}^{-}_{\mathrm{m}} \right). \tag{10}$$

After solving the micro-BVP problem, $\boldsymbol{\sigma}_{\mathrm{M}}$ can be recovered from the micro solution. For this end, the micro-to-macro upscaling procedure relies on the Hill-Mandel principle:

$$\boldsymbol{\sigma}_{\mathrm{M}} : \delta\boldsymbol{\varepsilon}_{\mathrm{M}} = \frac{1}{|\Omega_{\mathrm{m}}|} \int_{\Omega_{\mathrm{m}}} \boldsymbol{\sigma}_{\mathrm{m}} : \delta\boldsymbol{\varepsilon}_{\mathrm{m}}\, \mathrm{d}\Omega. \tag{11}$$

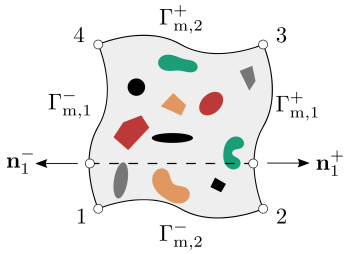


Figure 3. Periodicity of a 2D RVE (adapted from [6]).

That is, at any state of the RVE in equilibrium, the macroscopic variation of work must be equal to the volume average of the microscopic variation of work over the RVE. If $\tilde{\mathbf{u}}_{\mathrm{m}}$ is chosen in such a way that the microscopic fluctuation field does not contribute to the microscopic work, the expression above can be rewritten as [7]:

$$\sigma^{\mathrm{M}}_{ij} = \frac{1}{|\Omega_{\mathrm{m}}|}\int_{\Omega_{\mathrm{m}}} \sigma^{\mathrm{m}}_{ij}\,\mathrm{d}\Omega = \frac{1}{|\Omega_{\mathrm{m}}|}\int_{\Gamma_{\mathrm{m}}} t^{\mathrm{m}}_i x^{\mathrm{m}}_j\,\mathrm{d}\Gamma, \tag{12}$$

in which the volume integral above has been replaced by a contour integral of the product between the traction, $\mathbf{t}_{\mathrm{m}}$, and $\mathbf{x}_{\mathrm{m}}$.

2.4 Finite element analysis of the RVE

The finite element analysis at the micro level (i.e. RVE) consists of the determination of the nodal displacements and element stresses due to the imposed boundary displacements given by eq. (10), which are known as Periodic Boundary Conditions (PBCs). These conditions relate the displacements of n_p pairs of nodes on opposing boundaries of the micro model located at coordinates $\mathbf{x}^+$ and $\mathbf{x}^-$. It is important to note that the consideration of PBCs requires that the opposing model boundaries have exactly the same discretization, as shown in Fig. 4.

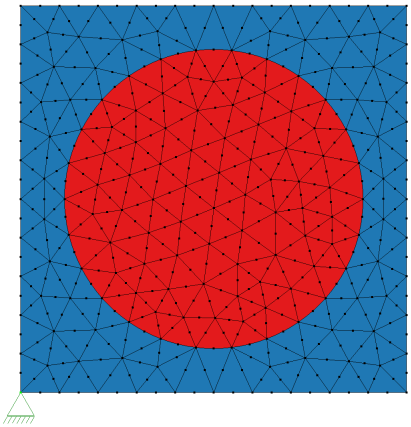


Figure 4. Finite element mesh of a 2D RVE.

The PBCs can be written as constraint equations relating the displacements of opposing nodes located at coordinates $\mathbf{x}^+$ and $\mathbf{x}^-$[9]:

$$\mathbf{u}^+_i - \mathbf{u}^-_i = (\mathbf{H}^{+T}_i - \mathbf{H}^{-T}_i)\,\boldsymbol{\varepsilon}_{\mathrm{M}}, \quad i = 1...n_p. \tag{13}$$

For 2D problems, these matrices are given by

$$\mathbf{H} = \frac{1}{2}\begin{bmatrix} 2x & 0 \\ 0 & 2y \\ y & x \end{bmatrix} \quad \text{and} \quad \boldsymbol{\varepsilon}_{\mathrm{M}} = \begin{bmatrix} \varepsilon_{xx} \\ \varepsilon_{xy} \\ \gamma_{xy} \end{bmatrix}. \tag{14}$$

These equations can be written in a more compact form as:

$$\mathbf{P}_i\,\mathbf{u} = \mathbf{Q}^T_i\,\boldsymbol{\varepsilon}_{\mathrm{M}}, \quad i = 1...n_p, \tag{15}$$

where $\mathbf{u}$ is the nodal displacement vector, $\mathbf{Q}_i = \mathbf{H}_i^+ - \mathbf{H}_i^-$, and $\mathbf{P}_i$ is a matrix whose entries consist only of $\{0, 1, -1\}$. Furthermore, the vertex displacements are given by:

$$\mathbf{P}_v \, \mathbf{u} = \mathbf{Q}_v^T \, \boldsymbol{\varepsilon}_{\mathrm{M}}, \quad v = 2...n_v, \tag{16}$$

where $\mathbf{Q}_v = \mathbf{H}_v$, and $\mathbf{P}_v$ is a matrix whose entries consist only of $\{0, 1\}$. The condition $\mathbf{u}_1 = \mathbf{0}$ is considered as an equality constraint since it can be easily enforced using simple supports, as depicted in Fig. 4. Finally, the constraint equations of all boundary nodes can be grouped and written in matrix form as:

$$\mathbf{P} \, \mathbf{u} = \mathbf{Q}^T \boldsymbol{\varepsilon}_{\mathrm{M}} \quad \Rightarrow \quad \mathbf{P} \, \mathbf{u} = \mathbf{b}. \tag{17}$$

The Lagrange Multiplier can be used to solve the equilibrium equations of the microscale model, considering the equality constraints presented in eq. (17). For instance, assuming a linear behavior, the unknown nodal displacements ($\mathbf{u}$) of the micro model can be obtained by the minimization of the Lagrangian function (L):

$$L = \frac{1}{2} \mathbf{u}^T \mathbf{K} \, \mathbf{u} + \boldsymbol{\mu}^T \left(\mathbf{P} \, \mathbf{u} - \mathbf{b} \right) \tag{18}$$

where $\mathbf{K}$ is the stiffness matrix and $\boldsymbol{\mu}$ are the Lagrange multipliers. The optimality conditions are:

$$\begin{aligned} \frac{\partial L}{\partial \mathbf{u}} &= \mathbf{K} \, \mathbf{u} + \mathbf{P}^T \, \boldsymbol{\mu} = \mathbf{0} \\ \frac{\partial L}{\partial \boldsymbol{\mu}} &= \mathbf{P} \, \mathbf{u} - \mathbf{b} = \mathbf{0} \end{aligned} \tag{19}$$

This approach can be easily extended to nonlinear problems, where the optimality conditions can be written as

$$\begin{aligned} \mathbf{r} &= \mathbf{g} + \mathbf{P}^T \, \boldsymbol{\mu} = \mathbf{0} \\ \mathbf{h} &= \mathbf{P} \, \mathbf{u} - \mathbf{b} = \mathbf{0} \end{aligned} \tag{20}$$

where $\mathbf{g}$ is the internal force vector. Details of the solution of these nonlinear equations using the Newton-Raphson method and the computation of the macroscopic stresses ($\boldsymbol{\sigma}_{\mathrm{M}}$) and macroscopic tangent constitutive matrix ($\mathbf{C}_{\mathrm{M}}$) are presented in [9].

3 Software Architecture

The proposed FE^2 was implemented in FAST (Finite element AnalySis Tool), which is an academic open-source FEM code developed at Universidade Federal do Ceará, written in C++ programming language using the object-oriented programming (OOP) paradigm. The original software architecture had to be modified to handle the creation and processing of nested finite element models. This was achieved by defining all data structures related to the finite element model, as well as local element and global routines, in appropriate classes. In FAST, these classes are *cModel* and *cControl*. Additional classes were created to implement the analysis of the microscale RVE. Fig. 5 illustrates the class diagram of the FAST software, with additional classes required for the FE^2 highlighted.

The *cModel* class stores mesh data, as nodes, elements (incidences and type) and its attributes (loads, boundary conditions, and material properties), using arrays and linked lists. The element object (*cElement*) is composed of a shape object (*cShape*), which stores node incidence and implements the shape functions and their derivatives evaluation, an analysis model object (*cAnModel*), which defines the degree of freedom of each node and strain-displacement relation, the section object (*cSection*), which stores section data and performs integration over thickness in plate and shell models, and the material object (*cMaterial*), used to store material parameters. The integration point (*cIntPoint*) class provides routines for quadrature creation, which are stored in each element object. Lastly, the constitutive model object (*cConstModel*) defines the stress-strain relation and constitutive matrix, defined respectively by the interface methods *Stress* and *CMatrix*, and stores and updates the material point state for nonlinear analysis. It is important to note that a constitutive model object is created for each integration point.

The *cControl* class implements numerical solvers for different analysis schemes, as linear static (*cLinStat*), nonlinear static based on Newton-Raphson iterations (*cCtrlNR*), or using path-following methods (*cCtrlPath*) as Arc Length. The first modification required for FE² module was the creation of solvers for the microscale problem. The *cCtrlMicroLin* class implements linear RVE analysis while *cCtrlMicroNL* implements nonlinear RVE analysis.

The solver method in these classes implements the analysis procedure detailed in section 2.4. The PBCs constraint coefficients are evaluated in the method *InitBC*. Two post-processing routines are used to compute

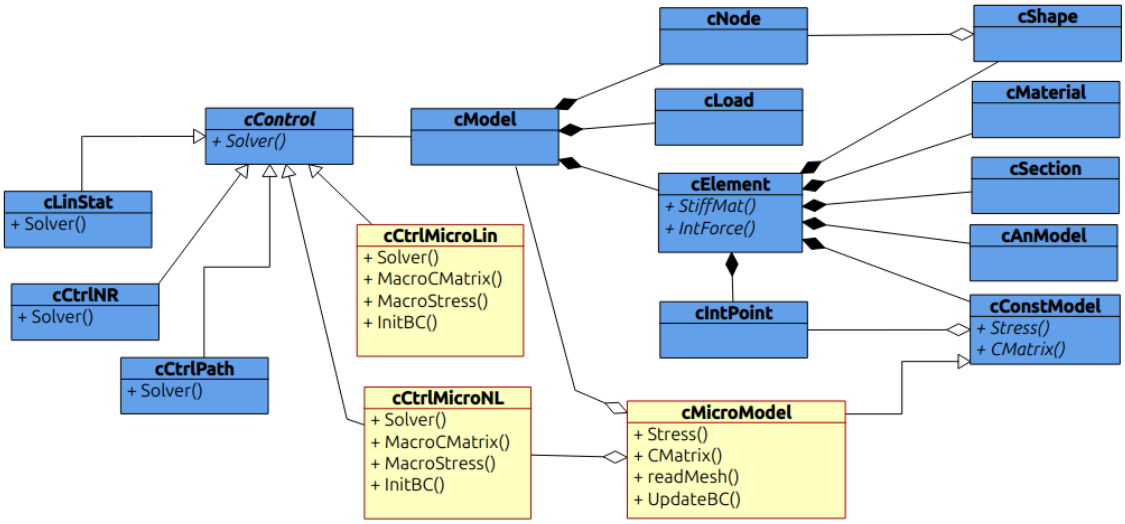


Figure 5. Class diagram of FAST software.

macroscale stresses ($\boldsymbol{\sigma}_{\mathrm{M}}$) and homogenized constitutive matrix ($\mathbf{C}_{\mathrm{M}}$), respectively, the methods *MacroStress* and *MacroCMatrix*. It is worth pointing out that this solver can be used to obtain effective properties of heterogeneous materials.

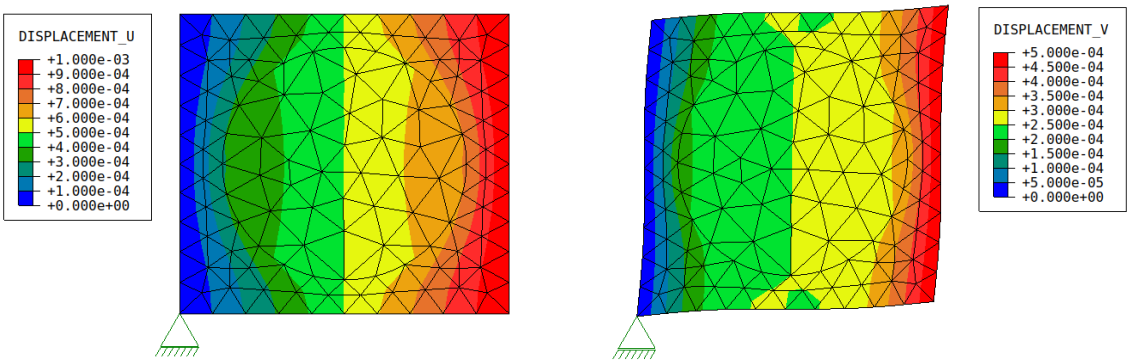
To implement FE^2 method, the class *cMicroModel* is used, which is a specialization of *cConstModel*. This class encapsulates the local finite element model and solver algorithm, which are created appropriately in its constructor. The micro model mesh read once from an input file using *readMesh*, and can be constant or vary across many instances of *cMicroModel*. The concrete implementation of *Stress* method processes the solver algorithm of *cCtrlMicro* and *cCtrlMicroNL* to evaluate macroscale stresses and homogenized constitutive matrix from the given strain at each integration point of the macroscopic model.

4 Numerical Results

The formulation presented in this work concerning the microscale analysis was implemented in FAST, in the solver object *cCtrlMicroLin*.

In order to verify the implementation, the elastic properties of a composite with boron fibers ($E = 379.3\,\mathrm{GPa}$ and $\nu = 0.1$) embedded in a aluminum matrix ($E = 68.3\,\mathrm{GPa}$ and $\nu = 0.3$) and fiber volume fraction equal to 0.47 [10] were computed using a RVE discretized in a mesh with 290 quadratic triangular elements (T6) and 621 nodes shown in Fig. 4. The plane strain condition was adopted since the cylindrical fibers are long.

The RVE was to subjected to the macroscopic strain fields: $\varepsilon_{\mathrm{M}_1} = [10^{-3}, 0, 0]^T$ and $\varepsilon_{\mathrm{M}_2} = [0, 0, 10^{-3}]^T$. Fig. 6 shows the deformed configurations obtained for these macroscopic strains. It can be noted that the RVE edges remain straight for $\varepsilon_{\mathrm{M}_1}$, but became curved for $\varepsilon_{\mathrm{M}_2}$. In both cases, the PBC are correctly enforced.



(a) Displacement u for $\varepsilon_{\mathrm{M}_1}$.

(b) Displacement v for $\varepsilon_{\mathrm{M}_2}$.

Figure 6. RVE displacement field (scale factor = 100).

The effective elastic properties in the direction perpendicular to the fibers were computed from the homogenized macroscopic constitutive matrix ($\mathbf{C}_{\mathrm{M}}$), and the obtained results are presented in Table 1. It is important to note that the same $\mathbf{C}_{\mathrm{M}}$ matrix was obtained for $\varepsilon_{\mathrm{M}_1}$ and $\varepsilon_{\mathrm{M}_2}$, since both materials were considered as linear elastic. The numerical results obtained in this work are in very good agreement with the reference values [10], showing the consistency of the mathematical formulation and its computer implementation.

Table 1. Elastic module for boron/aluminum composite (fiber volume fraction = 0.47).

Property	E_2 (GPa)	G_{23} (GPa)	ν_{23}
This work	147.7	45.8	0.29
Sun and Vaidya (1996)	144.0	45.9	0.29

5 Conclusion

This work presents the formulation of a computational homogenization technique and proposes an object-oriented software architecture for a finite element code to implement it. The implemented microscale analysis module was successfully verified with a numerical example available in the literature. The next step of this work is the implementation of nonlinear microscale analysis and the microscale constitutive model object in FAST.

Acknowledgements. The financial support by CNPq (Conselho Nacional de Desenvolvimento Científico e Tecnológico) and FUNCAP (Fundação Cearense de Apoio ao Desenvolvimento Científico e Tecnológico) are gratefully acknowledged

Authorship statement. The authors hereby confirm that they are the sole liable persons responsible for the authorship of this work, and that all material that has been herein included as part of the present paper is either the property (and authorship) of the authors, or has the permission of the owners to be included here.

References

[1] O. Pierard, C. Friebel, and I. Doghri. Mean-field homogenization of multi-phase thermo-elastic composites: a general framework and its validation. *Composites Science and Technology*, vol. 64, n. 10–11, pp. 1587–1603, 2004.

[2] J. Aboudi, S. Arnold, and B. Bednarcyk. *Micromechanics of Composite Materials*. Butterworth-Heinemann, Oxford, 2013.

[3] W. Ogierman. Data-driven mean-field homogenization: Enhancing the accuracy of the Mori-Tanaka method. *Composite Structures*, vol. 358, pp. 118985, 2025.

[4] M. Geers, V. Kouznetsova, and W. Brekelmans. Multi-scale computational homogenization: Trends and challenges. *Journal of Computational and Applied Mathematics*, vol. 234, n. 7, pp. 2175–2182. Fourth International Conference on Advanced COmputational Methods in ENgineering (ACOMEN 2008), 2010.

[5] D. Perić, E. A. de Souza Neto, R. A. Feijóo, M. Partovi, and A. J. C. Molina. On micro-to-macro transitions for multi-scale analysis of non-linear heterogeneous materials: unified variational basis and finite element implementation. *International Journal for Numerical Methods in Engineering*, vol. 87, n. 1-5, pp. 149–170, 2011.

[6] V. P. Nguyen. *Multiscale failure modelling of quasi-brittle materials*. Ph.d. dissertation, Delft University of Technology, 2011.

[7] V. G. Kouznetsova, W. A. M. Brekelmans, and F. P. T. Baaijens. An approach to micro-macro modeling of heterogeneous materials. *Computational Mechanics*, vol. 27, pp. 37–48, 2001.

[8] R. J. M. Smit, W. A. M. Brekelmans, and H. E. H. Meijer. Prediction of the mechanical behavior of nonlinear heterogeneous systems by multi-level finite element modeling. *Computer Methods in Applied Mechanics and Engineering*, vol. 155, n. 1, pp. 181–192, 1998.

[9] C. Miehe and A. Koch. Computational micro-to-macro transitions of discretized microstructures undergoing small strains. *Archive of Applied Mechanics*, vol. 72, pp. 300–317, 2002.

[10] C. T. Sun and R. S. Vaidya. Prediction of composite properties from a representative volume element. *Composites Science and Technology*, vol. 56, n. 2, pp. 171–179, 1996.